Tuning of the Mesogenic, Electronic, and Optical Properties of New Conjugated 3,3′-Bipyridine Derivatives

André-Jean Attias,*,[†] Philippe Hapiot,[‡] Véronique Wintgens,[§] and Pierre Valat[§]

ONERA, Département des Matériaux et Systèmes Composites, 29, Avenue de la Division Leclerc., B. P. 72, F-92322 Châtillon Cedex, France; Laboratoire d'Electrochimie Moléculaire de l'Université Denis Diderot-Paris 7, Unité Mixte de Recherche Université-CNRS No. 7591, Case Courrier 7107, 2, place Jussieu, F-75251 Paris Cedex 05, France; and CNRS, Laboratoire des Matériaux Moléculaires, 2-8, rue Henri-Dunant, F-94320 Thiais, France

We present two series of new 6,6′-distyryl-3,3′-bipyridine derivatives synthesized via a Knoevenagel condensation reaction of 6,6′-dimethyl-3,3′-bipyridine in the first series, and 5,5′,6,6′-tetramethyl-3,3′-bipyridine in the second one, with aromatic aldehydes para-substituted with electron donor or acceptor groups. These molecules were characterized by spectroscopic methods (NMR, UV−vis, photoluminescence), and cyclic voltammetry. Some compounds were found to exhibit thermotropic liquid crystalline (LC) phases, whose structures were analyzed by DSC and optical microscopy. The effects of molecular design on the mesogenic behavior, redox potentials, and fluorescence (nature and lifetimes of the excited states) were investigated. The high degree of conjugation and the mesogenic character of these molecules can lead to nonlinear optical (NLO) applications for the "push−pull" compounds. Absorption in the UV range and high fluorescence are other characteristics of some members of this group. The latter property, associated with high electron affinity, opens up light-emitting diode (LEDs) applications.

1. Introduction

π-Conjugated organic compounds have emerged as a promising class of advanced materials because of their large and fast second-order and third-order optical nonlinearities,[1,4] and/or of their fluorescence efficiency and semiconducting properties which have been exploited most notably in the development of efficient light emitting diodes (LEDs).[5] In all cases, the strong coupling between geometry and electronic structure is the source of the fascinating physics of these π-conjugated molecules and macromolecules.[6]

More precisely, large second-order optical nonlinearity is exhibited by noncentrosymmetric π-conjugated molecules containing an electron-acceptor group and an electron-donor group connected by an electron transmitting bridge. The π-conjugated cores are usually unsaturated moieties such as polyenes, stilbenes, and tolanes, or five-membered heteroatomic rings, such as thiophene.[7] Molecular configuration, variation in the relative strengths of the donor and acceptor groups, conjugation length, and nature of the π-electron system have well-established effects on the value of the first hyperpolarizability β.[8−10] For the successful construction of efficient polymer-based second-order nonlinear optical (NLO) materials, the crucial synthetic challenge is to maximize the number density of constituent high-β chromophore units while inducing and stabilizing maximum acentricity (unidirectional alignment) of the microstructure. In this regard, considerable progress has been made in the area of poled NLO polymers. The field has rapidly progressed from the first chromophore−polymer guest−host systems, to chromophore-functionalized side-chain polymers (SCPs). Recent investigations[11−19] have dem-

* Correspondence should be addressed to: A. J. Attias, O.N.E.R.A. Département des Matériaux et Systèmes Composites, 29 Avenue de la Division Leclerc, P. 72, F 92322 Châtillon Cedex, France. Telephone: (+33) 1 46 73 45 72. Fax: (+33) 1 46 73 41 42. E-mail: attias@onera.fr.
    † ONERA, Département des Matériaux et Systèmes Composites.
    ‡ Laboratoire d'Electrochimie Moléculaire de l'Université Denis Diderot-Paris 7.
    § CNRS, Laboratoire des Matériaux Moléculaires.

(1) Prasad, P. N.; Williams, D. J. In *Introduction to Nonlinear Optical Effects in Molecules and Polymers*; John Wiley: New York, 1991.
(2) Nalwa, H. S.; Seizo, M. In *Nonlinear Optics of Organic Molecules and Polymers*; CRC Press: Boca Raton, FL, 1994.
(3) Marder, S. R.; Torruellas, W. E.; Blanchard-Desce, M.; Ricci, V.; Stegeman, G. I.; Gilmour, S.; Brédas, J. L.; Li, J.; Bublitz, G. U.; Boxer, S. G. *Science* **1997**, *276*, 1233.
(4) Zyss, J. In *Molecular Nonlinear Optics: Materials, Physics and Devices*; Academic Press: New York, 1994.
(5) Burroughes, J. H.; Bradley, D. D. C.; Brown, A. R; Marks, R. N.; MacKay, K; Friend, R. H.; Burn, P. L.; Holmes, A. B. *Nature* **1990**, *347*, 539.
(6) Brédas, J. L. *Science* **1994**, *263*, 487.
(7) Varanasi, P. R.; Jen, A. K.-Y.; Chandrasekhar, J.; Namboothiri, I. N. N.; Rathna, A. *J. Am. Chem. Soc.* **1996**, *118*, 12443.
(8) Burland, D. M. *Optical Nonlinearities in Chemistry. Chem. Rev.* **1994**, *94* (special issue).
(9) Cheng, L. T.; Tam, W.; Stevenson, S. H.; Meredith, G. R.; Rikken, G.; Marder, S. R. *J. Phys. Chem.* **1991**, *95*, 10631.
(10) Cheng, L. T.; Tam, W.; Marder, S. R.; Stiegman, A. E.; Rikken, G.; Spangler, C. W. *J. Phys. Chem.* **1991**, *95*, 10643.
(11) Meredith, G. R.; Van Dusen, J. G.; Williams, D. J. *Macromolecules* **1982**, *15*, 1385.
(12) Singer, K. D.; Kuzyk, M. G.; Sohn, J. E. *J. Opt. Soc. Am. B: Opt. Phys.* **1987**, *4*, 968.
(13) Van der Vorst, C. P. J. M.; Picken, S. J. *Proc. SPIE* **1987**, *866*, 99.

onstrated that large second-order NLO effects can be obtained from side-chain polymers in which the NLO moieties possess the mesogenic properties by themselves,[15−20] leading to efficient side-chain liquid crystal polymers (SCLCPs). It is noticeable that the factors which enhance the second-order NLO activity of the molecules (high axial ratio, planarity, charged end groups) are essentially the same which favor the liquid crystal properties in low molar mass compounds.

Another interesting field of conjugated materials appears when considering the recent development of polymer-based LEDs.[21] In this connection, the interest for the modification of the conjugated backbones by chemical derivatization with π-electron donor and/or acceptor groups was recently underlined. The substitution allows an efficient control of the electronic parameters which are of importance for determining the device and the light emission characteristics, namely the band gap, the ionization potential and the electron affinity. For example, simultaneous derivatizations by alkoxy groups on the phenyl rings and cyano groups on the vinylene units of poly(paraphenylene vinylene) were found to increase significantly the electron affinity of the polymer.[21,22] This allows the electrodes made from air-stable metals such as aluminum to be used for electron injection, while decreasing the ionization potential. In this connection, recent results demonstrate that because the high-electron affinity of the pyridine ring, pyridine-based conjugated polymers can also be used in LEDs made from environmentally stable metal electrodes.[23−28] Conjugated low molar mass oligomers possessing well-defined conjugation lengths and structures also have been the subject of increasing attention in the last years because of their ability to give high purity films by vacuum deposition[29,30] and also because they can serve as model systems for understanding the relationships between bulk material properties and molecular structures in the parent polymers.[26,31]

As evidenced from the above narrative, it is a challenge for the chemist to design conjugated molecules possessing mesogenic properties by themselves, as well as high electron affinity, and presenting intramolecular charge transfer state. This affords the opportunity for a fine-tuning of the system properties. The aim of the present work is to propose a new efficient π-conjugated core and the associated synthetic pathway to enlarge the number of available compounds.

In this field, we have described, in a previous paper,[32] a strategy to synthesize by means of the Knoevenagel condensation:
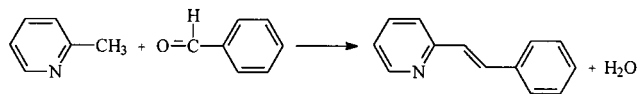
a series of 6,6′-distyryl-3,3′-bipyridine derivatives (**A1−5**) (see Tables 1−3 for structures) as a new class of liquid crystalline conjugated molecules. These compounds are prepared by reaction of 6,6′-dimethyl-3,3′-bipyridine (**A0**) with aromatic aldehydes, e.g., thiophene or benzene rings substituted with electron acceptor or donor groups. These preliminary results have shown that these compounds exhibit, in addition to mesomorphism, absorption in the UV spectral range, and, in solution, intense emission in the blue region.

The major interests for liquid crystals and side-chain liquid crystal polymers are motivated by their spontaneous tendency to a high degree of axial ordering and consequently their easy coupling to an external field,[18,33,34] more particularly in the case of the less viscous smectic A and nematic phases. However, all the previously investigated compounds exhibit mesophases with high transition temperatures. Especially, nematic phases occur at temperatures not very far from degradation or sublimation points. To favor the occurrence of the highly fluid nematic phase, we have to lower the transition temperatures to prevent any thermal degradation during macroscopic alignments of liquid crystals.

In the present work, to achieve this goal, methyl groups have been introduced, as lateral substituents into the pyridinic rings of the molecules of the **A** series into the 5 and 5′-positions of the 6,6′-dimethyl-3,3′-bipyridine, giving the homologous series **B**. In this paper, we report the synthesis of a series of 5,5′-dimethyl-6,6′-distyryl-3,3′-bipyridine derivatives (**B1−5**) (see Tables 1−3 for structures) and compare the mesogenic, electrochemical, and photophysical properties for the two series of molecules (**A1−5** and **B1−5**). They were characterized by means of ¹H and ¹³C NMR spectroscopies, differential scanning calorimetry (DSC), optical microscopy, X-ray diffraction, cyclic voltametry,

(14) Van der Vorst, C. P. J. M.; Picken, *S. J. J. Opt. Soc. Am.* **1990**, *B7*, 320.

(15) Gonin, D.; Noël, C.; Le Borgne, A.; Gadret, G.; Kajzar, F. *Makromol. Chem., Rapid Commun.* **1992**, *13*, 537.

(16) Guichard, B.; Noël, C.; Reyx, D.; Kajzar, F. *Macromol. Chem. Phys.* **1996**, *197*, 2185.

(17) Guichard, B.; Poirier, V.; Noël, C.; Reyx, D.; Le Borgne, A.; Leblanc, M.; Large, M.; Kajzar, F. *Macromol. Chem. Phys.* **1996**, *197*, 3631.

(18) Gonin, D.; Guichard, B.; Noël, C.; Kajzar, F. In *Polymers and Other Advanced Materials: Emerging Technologies and Business Opportunities*; Prasad, P. N., et al., Eds.; Plenum Press: New York, 1995; pp 465−483.

(19) Gonin, D.; Guichard, B.; Large, M.; Dantas De Morais, T.; Noël, C.; Kajzar, F. *J. Nonlinear Opt.l Phy. Mater.* **1996**, *5*, 735.

(20) Dubois, J. C.; Le Barny, P.; Mauzac, M.; Noël, C. *Polymer* **1997**, *48*, 47.

(21) (a) Brédas, J. L.; Heeger, A. J. *Chem. Phys. Lett.* **1994**, *217*, 507. (b) *IEEE J. Sel. Top. Quantum Electron.* **1998**, *4*. (c) Tessler, N. *Adv. Mater.* **1999**, *11*, 363.

(22) Greenham, N. C.; Moratti, S. C.; Bradley, D. D. C.; Friend, R. H.; Holmes, A. B. *Nature* **1993**, *365*, 628.

(23) Marsella, M. J.; Fu, D. K.; Swager, T. M. *Adv. Mater.* **1995**, *7*, 145.

(24) Epstein, A. J.; Blatchford, J. W.; Wang, Y. Z.; Jessen, S. W.; Gebler, D. D.; Lin, L. B.; Gustafson, T. L.; Wang, H. L.; Park, Y. W.; Swager, T. M.; MacDiarmid, A. G. *Synth. Met.* **1996**, *78*, 253.

(25) Blatchford, J. W.; Jessen, S. W.; Lin, L. B.; Lih, J. J.; Gustafson, T. L.; Epstein, A. J.; Fu, D. K.; Marsella, M. J.; Swager, T. M.; MacDiarmid, A. G.; Yamaguchi, S.; Hamaguchi, H. *Phys. Rev. Lett.* **1996**, *76*, 1513.

(26) Wang, Y. Z.; Gebler, D. D.; Fu, D. K.; Swager, T. M.; MacDiarmid, A. G.; Epstein, A. J. *Synth. Met.* **1997**, *85*, 1179.

(27) Gebler, D. D.; Wang, Y. Z.; Jessen, S. W.; Blatchford, J. W.; MacDiarmid, A. G.; Swager, T. M.; Fu, D. K.; Epstein, A. J. *Synth. Met.* **1997**, *85*, 1205.

(28) Cornil, J.; Beljonne, D.; Dos Santos, D. A.; Shuai, Z.; Bredas, J. L. *Synth. Met.* **1996**, *78*, 209.

(29) Hosokawa, C.; Higashi, H.; Kusumoto, T. *Appl. Phys. Lett.* **1993**, *62*, 3238.

(30) Adachi, C.; Tsutsui, T.; Saito, S. *Appl. Phys. Lett.* **1990**, *56*, 799.

(31) Maddux, T.; Li, W.; Yu, L. *J. Am. Chem. Soc.* **1997**, *119*, 844.

(32) Attias, A.-J.; Cavalli, C.; Bloch, B.; Guillou, N.; Noël, C. *Chem. Mater.* **1999**, *11*, 2057.

(33) De Gennes, P. G. *The Physics of Liquid Crystals*; Clarendon Press: Oxford, 1974.

(34) Blinov, L. M. *Electro-optical and Magneto-optical Properties of Liquid Crystals*; Wiley Interscience: New York, 1983.

and UV−visible and fluorescence spectroscopies. Specific properties which are of interest are (i) the changes in the thermal transitions and liquid crystalline behavior, (ii) redox potentials (used to estimate the relative ionization potentials and electron affinities), and (iii) the following optical properties: absorption and emission spectra (both in solution and in solid state), Stokes shifts, emission quantum yields, and lifetimes of the excited states. Solvatochromic effects on fluorescence have been also investigated, to evidence intramolecular charge transfer. In all cases the properties were analyzed and discussed in terms of nature of the conjugated core and end-substituent effects.

2. Experimental Section

2.1. Reagents. Standard methods have been used to synthesize 2-methyl-5-bromopyridine[35] and 2,3-dimethyl-5-bromopyridine.[36] Benzoic anhydride, benzaldehyde, 4-cyano-benzaldehyde, 4-hexyloxybenzaldehyde, and 2-thiophenecar-boxaldehyde (all from Aldrich) were used without further purification.

2.2. Syntheses. The syntheses and analytical characteristics of 6,6′-dimethyl-3,3′-bipyridine, and of compounds **A1**−**5** have been previously reported.[32]

5,5′,6,6′-Tetramethyl-3,3′-bipyridine (B0). A total of 14.16 g of nickel(II) chloride hexahydrate (60 mmol), 62.4 g of triphenylphosphine (240 mmol), and 300 mL of *N,N*-dimethylformamide were introduced into a three-necked flask fitted with a condenser, a dropping funnel, and an argon inlet. The resulting deep blue solution was then stirred for 1 h at 50 °C, and 3.84 g of zinc powder (60 mmol) was added. After 1 h, the color of the reaction mixture has changed to red brown. A total of 11.16 g of 2,3-dimethyl-5-bromopyridine (60 mmol) was then added, and the reaction progress was monitored by steric exclusion chromatography (SEC). After 10 h, 2,3-dimethyl-5-bromopyridine was consumed. The mixture was cooled to room temperature, then poured into 600 mL of a dilute ammonia solution, and extracted four times with dichloromethane (4 × 120 mL). The resulting organic phase was extracted with a 2 M HCl solution (3 × 150 mL). The aqueous phase was made alkaline with a 4 M NaOH solution, and the reaction product was extracted with dichloromethane (3 × 120 mL). The organic phase was washed with water. After evaporation, 5.2 g of a crude product was obtained and purified by vacuum sublimation. A total of 4.8 g (23 mmol) of pure 5,5′,6,6′-tetramethyl-3,3′-bipyridine (**B0**) was obtained as a white pinkish powder (yield 76%): mp 218 °C; ^{1}H NMR (CDCl$_3$) δ [ppm] 2.34 (s, 6H), 2.53 (s, 6H), 7.56 (d, 2H, ^4J(H,H) = 2.15 Hz), and 8.50 (d, 2H, ^4J(H,H) = 2.15 Hz); ^{13}C NMR (CDCl$_3$) δ [ppm] 19.2, 22.3, 131.2, 131.5, 135.3, 144.5, and 156.5. Anal. Calcd for C$_{14}$H$_{16}$N$_2$: C, 79.21; H, 7.6; N, 13.2. Found: C, 79.46; H, 7.58; N, 12.96.

5,5′-Dimethyl-6,6′-distyryl-3,3′-bipyridine (B1). A total of 3.18 g (15 mmol) of 5,5′,6,6′-tetramethyl-3,3′-bipyridine (**B0**), 6.5 g (63 mmol) of benzaldehyde, and 7.9 g (35 mmol) of benzoic anhydride were introduced into a three-necked flask fitted with a condenser, a dropping funnel, and an argon inlet. The mixture was then stirred at 150 °C, and the reaction's progress was monitored by SEC. After 4 h, 5,5′,6,6′-tetramethyl-3,3′-bipyridine was consumed. The mixture was cooled to room temperature and washed with a 2 N NaOH solution to eliminate excess of benzoic anhydride and acid formed during the reaction. The crude product was crystallized twice from ethanol. A total of 2.67 g (6.9 mmol) of 5,5′-dimethyl-6,6′-distyryl-3,3′-bipyridine was obtained as yellow powder (yield 46%): mp 211.5 °C; ^{1}H NMR (CDCl$_3$) δ [ppm] 2.53 (s, 6H), 7.32 (d, 2H, ^3J(H,H) = 7.30 Hz), 7.38 (d, 2H, ^3J(H,H) = 15.6 Hz), 7.39 (dd, 4H, ^3J(H,H) = 7.3 Hz, ^3J(H,H) = 7.3 Hz), 7.63

(d, 4H, ^3J(H,H) = 7.3 Hz), 7.67 (d, 2H, ^4J(H,H) = 2.15 Hz), 7.86 (d, 2H, ^3J(H,H) = 15.6 Hz), and 8.73 (d, 2H, ^4J(H,H) = 2.15 Hz); ^{13}C NMR (CDCl$_3$) δ [ppm] 19.0, 123.5, 127.2, 128.3, 128.7, 130.8, 131.5, 134.1, 136.0, 137.0, 145.2, and 152.9. Anal. Calcd for C$_{28}$H$_{24}$N$_2$: C, 86.56; H, 6.23; N, 7.21. Found: C, 86.51; H, 6.28; N, 7.21.

5,5′-Dimethyl-6,6′-bis(2-thienyl vinylene)-3,3′-bipyridine (B2). This compound was prepared by the same procedure, but from 2-thiophenecarboxaldehyde (yield 40%): mp 175 °C; ^{1}H NMR (CDCl$_3$) δ [ppm] 2.50 (s, 6H), 7.04 (dd, 2H, ^3J(H,H) = 5.1 Hz, ^3J(H,H) = 3.44 Hz), 7.17 (d, 2H, ^3J(H,H) = 15.6 Hz), 7.22 (d, 2H, ^3J(H,H) = 3.44 Hz), 7.27 (d, 2H, ^3J(H,H) = 5.1 Hz), 7.65 (d, 2H, ^4J(H,H) = 2.28 Hz), 7.98 (d, 2H, ^3J(H,H) = 15.6 Hz), and 8.69 (d, 2H, ^4J(H,H) = 2.28 Hz); ^{13}C NMR (CDCl$_3$) δ [ppm] 19.0, 122.5, 125.4, 126.9, 127.7, 128.0, 130.5, 131.1, 135.8, 142.4, 144.9, and 152.4. Anal. Calcd for C$_{24}$H$_{20}$N$_2$S$_2$: C, 71.97; H, 5.03; N, 6.99; S, 16.01. Found: C, 71.94; H, 5.04; N, 7.02.

5,5′-Dimethyl-6,6′-bis(4-cyanostyryl)-3,3′-bipyridine (B3). This compound was prepared by the same procedure, but from 4-cyanobenzaldehyde (yield 86%): ^{1}H NMR (CDCl$_3$) δ [ppm] 2.56 (s, 6H), 7.49 (d, 2H, ^3J(H,H) = 15.34 Hz), 7.68 (s, 4H), 7.69 (s, 4H), 7.72 (d, 2H, ^4J(H,H) = 2.56 Hz), 7.87 (d, 2H, ^3J(H,H) = 15.34 Hz), 8.75 (d, 2H, ^4J(H,H) = 2.56 Hz); ^{13}C NMR (CDCl$_3$) δ [ppm] 19.0, 111.3, 118.5 (*C*N), 118.9, 126.6, 127.4, 131.4, 131.9, 132.3, 136.1, 141.2, 145.2, and 151.7. Anal. Calcd for C$_{30}$H$_{22}$N$_4$: C, 82.17; H, 5.06; N, 12.78. Found: C, 82.18; H, 5.12; N, 12.70.

5,5′-Dimethyl-6,6′-bis(4-hexyloxystyryl)-3,3′-bipyridine (B4). This compound was prepared by the same procedure, but from 4-hexyloxybenzaldehyde (yield 42%): ^{1}H NMR (CDCl$_3$) δ [ppm] 0.91 (t, 6H, ^3J(H,H) = 6.75 Hz), 1.34 (m, 8H), 1.45 (m, 4H), 1.8 (m, 4H), 2.51 (s, 6H), 3.98 (t, 4H, ^3J(H,H) = 6.75 Hz), 6.92 (d, 4H, ^3J(H,H) = 8.64 Hz), 7.24 (d, 2H, ^3J(H,H) = 15.5 Hz), 7.56 (d, 4H, ^3J(H,H) = 8.64 Hz), 7.65 (d, 2H, ^4J(H,H) = 2.0 Hz), 7.81 (d, 2H, ^3J(H,H) = 15.5 Hz), and 8.71 (d, 2H, ^4J(H,H) = 2.0 Hz); ^{13}C NMR (CDCl$_3$) δ [ppm] 14.0, 19.0, 22.5, 25.6, 29.1, 31.6, 68.0, 114.6, 121.2, 128.5, 129.4, 130.3, 131.0, 133.5, 135.8, 144.9, 153.0, and 159.4. Anal. Calcd for C$_{40}$H$_{48}$N$_2$O$_2$: C, 81.59; H, 8.22; N, 4.76; O, 5.43. Found: C, 81.63; H, 8.24; N, 4.70.

5,5′-Dimethyl-6-(4-cyanostyryl)-6′-(4-hexyloxystyryl)-3,3′-bipyridine (B5). This compound was prepared by the same procedure, but the synthesis was conducted in two steps, with equimolecular proportion of, successively, 4-cyanobenzaldehyde and 4-hexyloxybenzaldehyde. The intermediate compound resulting from the condensation of 5,5′,6,6′-tetramethyl-3,3′-bipyridine with 4-cyanobenzaldehyde (1/1 mol/mol) was isolated by dissolution in ethanol and purified before the condensation with 4-hexyloxybenzaldehyde (1/1 mol/mol) (yields: step1, 35%; step 2, 53%): ^{1}H NMR (CDCl$_3$) δ [ppm] 0.91 (t, 3H, ^3J(H,H) = 6.8 Hz), 1.35 (m, 4H), 1.47 (m, 2H), 1.8 (m, 2H), 2.52 (s, 3H), 2.55 (s, 3H), 3.99 (t, 2H, ^3J(H,H) = 6.8 Hz), 6.92 (d, 2H, ^3J(H,H) = 8.6 Hz), 7.23 (d, 1H, ^3J(H,H) = 15.6 Hz), 7.48 (d, 1H, ^3J(H,H) = 15.6 Hz), 7.56 (d, 2H, ^3J(H,H) = 8.6 Hz), 7.68 (m, 6H) *[7.66 (d, ^4J(H,H) = 2.1 Hz) − 7.67 (s) − 7.68 (s) − 7.70 (d, ^4J(H,H) = 2.1 Hz)]*, 7.82 (d, 1H, ^3J(H,H) = 15.6 Hz), 7.85 (d, 1H, ^3J(H,H) = 15.6 Hz), 8.71 (d, 1H, ^4J(H,H) = 2.1 Hz), and 8.74 (d, 1H, ^4J(H,H) = 2.1 Hz); ^{13}C NMR (CDCl$_3$) δ [ppm] 14.0, 18.9, 19.0, 22.5, 25.6, 29.2, 31.6, 68.1, 111.1, 114.5, 118.5 (*C*N), 118.7, 120.8, 126.8, 127.4, 128.5, 129.3, 130.3, 130.5, 131.3, 131.6, 132.3, 133.8, 135.8, 135.9, 141.3, 144.9, 145.2, 151.5, 153.5, and 159.4. Anal. Calcd for C$_{35}$H$_{35}$N$_3$O: C, 81.84; H, 6.87; N, 8.18; O, 3.11. Found: C, 81.79; H, 6.88; N, 8.22.

Techniques. *Nuclear Magnetic Resonance (NMR) Spectroscopy.* ^{1}H and ^{13}C NMR spectra were recorded on a Varian Unity 300 spectrometer operating at 299.95 and 75.144 MHz, respectively. Chloroform-*d* (CDCl$_3$) was used as solvent, and tetramethylsilane (TMS) as internal standard.

Thermal Analysis. The transition temperatures were measured using a differential thermal analyzer (Dupont 1090) operating at 20 °C/min under nitrogen.

Phase Behavior. Optical textures were observed under a polarizing microscope (Olympus BHA-P) equipped with a Mettler FP52 hot-stage and FP 5 control unit, or a Leitz 350

(35) Pearson, D. E.; Hargrove, W. W.; Chow, J. K. T.; Suthers, B. R. *J. Org. Chem.* **1961**, *26*, 789.

(36) Bonnier, J. M.; Court, J. *Bull. Soc. Chim. Fr.* **1970**, *1*, 142.

microscope (Ernst Leitz, Wetzlar) for observations in the temperature range 300−350 °C.

Optical Spectroscopies. The UV−visible absorbance spectra for compounds **A1**−**5** and **B1**−**5** were obtained from their solutions in a toluene/acetonitrile (50/50 v/v) mixture using a Lambda 18 UV−vis spectrometer (Perkin-Elmer). A 1-cm quartz cell was used. The concentrations were chosen so that appropriate absorbance values (0.1 to 0.2) were obtained at λ_{max}. The fluorescence and excitation spectra were obtained from the same solutions, using a Aminco S.L.M. 8100 luminescence spectrometer. Fluorescence quantum yields were measured in toluene/acetonitrile (50/50 v/v) solutions by comparison with the emission of quinine sulfate for which a value 0.55 has been taken.[37] Quantum yield were not corrected for the change in refractive index between the toluene/acetonitrile (50/50 v/v) solutions and aqueous sulfuric solution. The energy of the 0,0 transitions ($E_{0,0}$) was taken as the crossing point of the excitation and absorption spectra. Solid-state product was excited with polarized light; polarized emission was collected across a simple monochromator.

Cyclic Voltammetry. Electrochemistry experiments were performed with a three-electrode setup using a platinum counter electrode and a reference electrode. The reference electrode was an aqueous saturated calomel electrode with a salt bridge containing the supporting electrolyte. The working electrode was either disk of glassy carbon (diameter 0.8 mm, Tokai Corp.), gold (diameter 1 mm), or platinum (diameter 1 mm). The working electrodes were carefully polished before each set of voltammograms with 1 μm diamond paste and cleansed in an ultrasonic bath with dichloromethane. The electrochemical instrumentation consisted of a PAR model 175 Universal programmer and of a home-built potentiostat equipped with a positive feedback compensation device.[38] The data were acquired with a 310 Nicolet oscilloscope. The potential values were internally calibrated against the ferrocene/ferricinium couple ($E° = 0.405$ V vs SCE) for each experiment. All the cyclic voltammetry experiments were carried out at 20 °C using a cell equipped with a jacket allowing circulation of water from the thermostat. Oxygen was removed from all solutions by bubbling argon. The solvent was a toluene/acetonitrile mixture (50/50 v/v) and the supporting electrolyte was tetrabutylammonium tetrafluoroborate (Fluka, Puriss) at a concentration of 0.1 mol L^{-1}. Acetonitrile was from Merck (Uvasol quality less than 0.01% of water), and toluene, from Prolabo (R. P. Normapur).

3. Results and Discussion

3.1. Synthesis. The chromophores were obtained by Knoevenagel condensation, under acidic conditions, of 1 mol of **A0** (**B0**) with 2 mol of the appropriate aldehyde, leading to **A1**−**4** (**B1**−**4**). The synthesis of the unsymmetrically disubstituted molecules (**A5** and **B5**) required two steps: (i) condensation of **A0** (**B0**) with 4-cyanobenzaldehyde (1/1 mol/mol) and then (ii) condensing the intermediate compound with 4-hexyloxybenzaldehyde to yield **A5** (**B5**). The compounds were characterized and identified by ^{1}H and ^{13}C NMR spectroscopies and found to be analytically pure by elemental analyses.

In the case of the 6,6′-dimethyl-3,3′-bipyridine, the Knoevenagel-type condensation is made possible by activation of the methyl groups resulting from their ortho position with respect to the nitrogen atom. Concerning the 5,5′,6,6′-tetramethyl-3,3′-bipyridine, note that only the 6,6′-methyl groups are involved in the condensation; the methyl groups in the meta position with respect to the nitrogen atom are not being activated.

In all cases the trans stereochemistry of the double bond was well established by the coupling constant of the vinylic protons in the ^{1}H NMR spectra ($J^3_{HH} = 15−16$ Hz).

3.2. Mesomorphic Behavior. All the compounds were examined by DSC and phase assignments are based on powder X-ray diffraction (only for **A1**−**5**) and polarizing optical microscopy. The transition temperatures and the textures observations are listed in Table 1.

As detailed in the previous work,[32] **A1**−**5** form mesophases which were all identified. For example, **A1** has smectic A (S$_A$), nematic (N), and isotropic (I) phases, occurring at 240, 282.7, and 315.1 °C, respectively. Texture observation of this compound, under a polarizing microscope, shows, above the melting point, a typical focal−conic fan texture and a *Schlieren* texture, respectively for the S$_A$ and N phases. Compounds **A2**−**4** exhibit many crystalline modifications, not reported here.[32] The very powerful effect of the cyano and *n*-hexyloxy terminal groups in promoting nematic and smectic phase formation respectively, according to the literature,[39] is clearly evidenced with compounds **A3** and **A4**. This is highlighted by the fact that the unsymmetrically para-disubstituted molecule **A5** exhibits, in addition to a crystalline phase, two smectic phases (S$_B$ and S$_A$) and a nematic phase. The measurements reported in Table 1 indicate that all compounds exhibit mesophases whose transition temperatures are very high, more particularly for smectic A and nematic phases ($\geq$230 °C). Furthermore, the isotropization temperatures are above 290 °C in all cases.

Liquid crystalline properties of the new compounds **B1**−**5** are also reported in Table 1. **B1**−**2** do not exhibit any mesogenic behavior. The clearing temperatures of these two compounds, 211 and 175 °C respectively, are lower than for the analogous **A1**−**2** molecules, 315 and 291 °C, respectively. In contrast, compounds **B3**−**5** demonstrate LC phases. Texture observation by polarizing microscopy indicates that they all form only enantiotropically nematic *Schlieren* textures in the LC range. For example, **B4** is purely nematogenic, whereas the parent **A4** is purely smectogenic. The N/I transition occurs at 174 °C for **B4**, while the isotropization temperature for **A4** is undetected up to ∼315 °C, temperature at which sublimation and degradation occur. **B5** also possesses only a nematic phase, which is also the broadest. Comparison of the thermal behavior of **B5** with analogous structure **A5**, which exhibit smectic and nematic phases, indicates that **B5** has lower transition temperatures and less LC stability. **B3** displays a K/N transition at higher temperature (345 °C) than **A3** (311 °C), but the thermal stability of the N phase cannot be evaluated because degradation occurs before isotropization, as for **A3**.
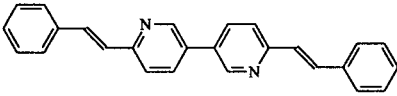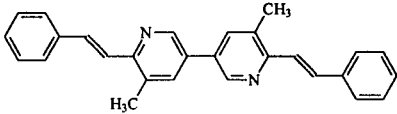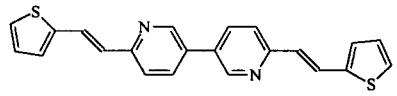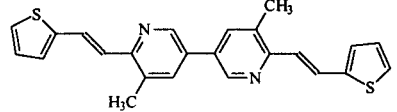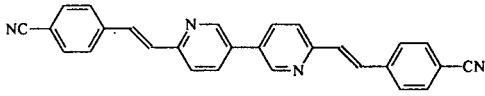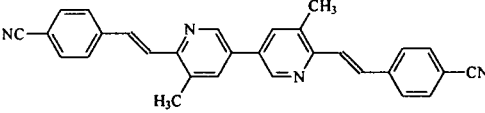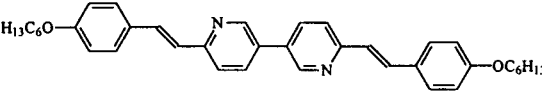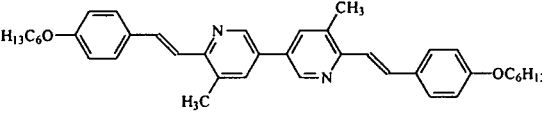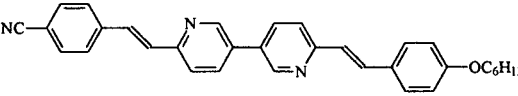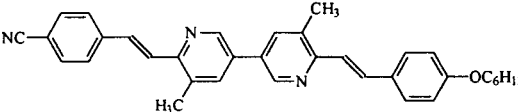
Comparison of the liquid crystal transition temperatures for compounds **B1**−**5**, with those of their homologous **A1**−**5** indicates that 5,5′-methyl substituents markedly decrease liquid crystal thermal stabilities: smectic phases are suppressed; the nematic phase

(37) Melhuish, W. H. *J. Phys. Chem.* **1961**, *65*, 229.
(38) Garreau, D.; Savéant, J.-M. *J. Electroanal.* **1972**, *35*, 309.

(39) Gray, G. W. In *Influence of Composition and Structure on the Liquid Crystals formed by Non-Amphiphilic Systems, in Liquid Crystals*; Gray, G. W., Winso, P. A., Eds.; Ellis Horwood Limited: Chichester, 1974; pp 103−152.

Table 1. Phases Transitions of Compounds A1–5 and B1–5[c]

Compound	K	S_F	S_B	S_C	S_A	N	I
					Transition temperature (°C)		
A1	[a] •				240 •	282.7 •	315.1 •
B1	•						211.5 •
A2	[a] •					263.4 •	291.3 •
B2	•						175 •
A3	[a] •					311.9 •	>350[b] •
B3	•					345.8 •	>350[b] •
A4	[a] •	164.3 •		204 •	251.1 •		>315[b] •
B4	•					130 •	174.4 •
A5	[a] •	120.7 •		185 - 205 •		233.7 •	302.5 •
B5	•					176 •	232 •

(Compound column contains the chemical structure drawings of A1–A5 and B1–B5; the B compounds bear lateral CH_3 substituents on the bipyridine core, with terminal groups: phenyl (1), 2-thienyl (2), NC-phenyl (3), $H_{13}C_6O$-phenyl (4), and mixed NC/OC_6H_{13} (5).)

[a] See ref 32. [b] Degradation and sublimation occur at and above. [c] Abbreviations: K, solid crystal; S_X, smectic X; N, nematic; I, isotropic liquid.

stability is substantially decreased. The reason for this is probably that the weakly dipolar lateral substituent CH_3 broadens the molecule and reduces the tendency of the compound to form liquid crystals.[39,40] This effect is more pronounced for molecules such as **B1** and **B2** which do not exhibit mesophases. This is probably due to the fact that they do not bear terminal substituents which favor the formation of smectic or nematic mesophases.

3.3. Optical Study. Absorption spectra were measured in ethyl acetate (AcOEt), DMF, and in toluene/acetonitrile mixture (TA) (50/50 v/v). AcOEt and DMF were selected for their very different dielectric constants ($\epsilon_{AcOEt} = 6.0$, $\epsilon_{DMF} = 36.7$) and TA to compare the results obtained in the optical and electrochemical studies, more particularly energy gaps. Photoluminescence experiments have been carried out for all compounds in AcOEt, DMF, TA, and in the solid state. For unsymmetrically disubstituted derivatives (**A5** and **B5**), fluorescence was also performed in pure solvents with different polarity.

3.3.1. Optical Study in Solution. Representative absorption and emission spectra for **A1–5** in TA are reported in Figure 1. The absorption and fluorescence

(40) Coates, D. In *Liquid Crystals, Applications and Uses*; Bahadur, B., Eds.; World Scientific: Singapore, 1990; pp 92–137.
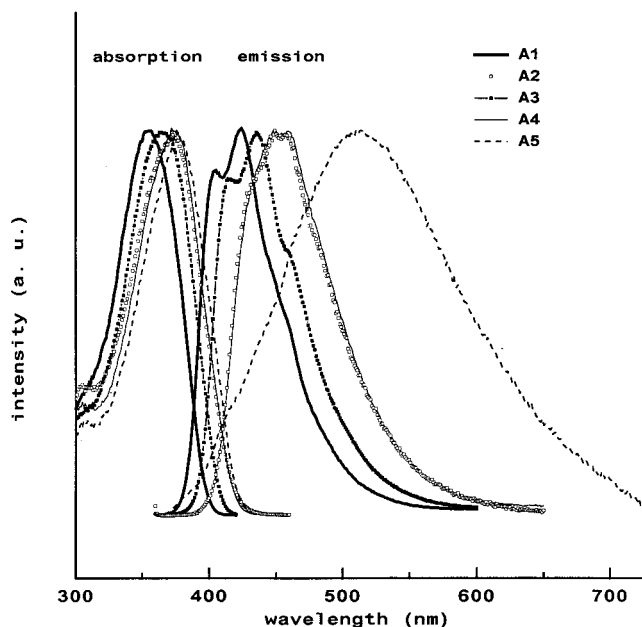
Figure 1. Absorption and emission spectra of **A1**−**5** in toluene/acetonitrile mixture (50/50 v/v). Intensities of spectra have been normalized to the same value.

spectra exhibit the same features for the two **A** and **B** series regardless of the solvent polarity and show no significant shift of the absorption and emission maxima (λ^a_{max} and λ^e_{max}) excepted a large solvatochromic effect observed for the emission for **A5** and **B5** (see below). All the optical data for **A1**−**5** and **B1**−**5**, measured in TA, are summarized in Table 2.

All the compounds, as shown in Figure 1, exhibit essentially the same absorption profile: an intense, low-lying (near UV region), and structureless absorption band. The large molar absorption coefficients ($\geq 30\,000$ L mol^{-1} cm^{-1}) are indicative of highly π-conjugated systems. Photoluminescence is observed for all the compounds in solution. The salient feature of the emission spectra is the appearance, for **A1**, **B1**, **A3**, and **B3**, and the absence for the other chromophores, of a structured emission. The energy of the emission maxima of **A5** and **B5** depends strongly on solvent polarity as shown in Figure 2. The only noticeable variations in absorption and emission maxima are (i) a red shift of the maxima wavelengths for compounds **A2**−**4** and **B2**−**4** compared to those of **A1** and **B1** respectively ($\Delta\lambda_{max} = 10$−20 nm), and (ii) a bathochromic shifts of λ_{max} for chromophores of series **A** compared to those of series **B** respectively ($\Delta\lambda_{max} = 5$−10 nm) as presented in Figure 3 for **A3** and **B3**. Such a red shift is consistent with the fact that the donating and withdrawing substituents of the pyridinic ring enhance the π-electron delocalization along the unsaturated system. As shown from the comparisons of **A4**, **A2**, and **B2** with **A1**, which absorb at 373, 377, 382, and 355 nm respectively, all the factors reinforcing the electronic density on the pyridinic ring (donor strength of the substituent: *n*-hexyloxy, or thienyl ring, or methyl lateral substituent) increases the values of the maxima wavelengths.
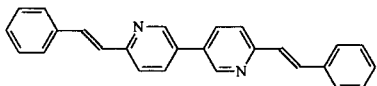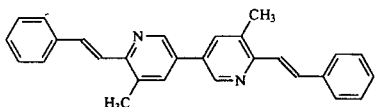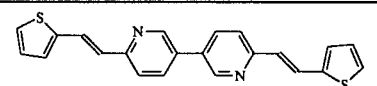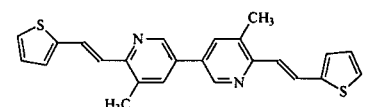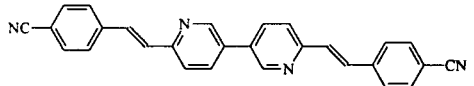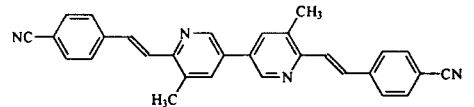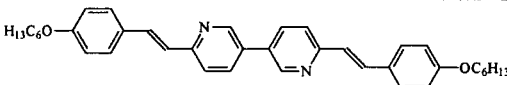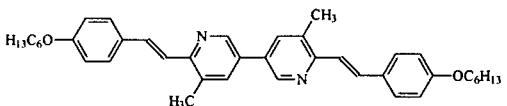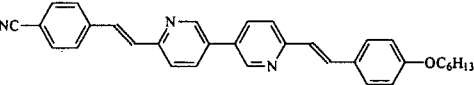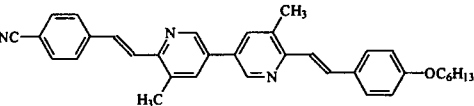
In addition to the effects on the absorption and emission energies, the nature of the conjugated core and of the end substituents also influences the emission band shape, Stokes shift, quantum yield (Φ_f), and lifetime (τ_f) of the chromophores.

As shown in Figure 1, the asymmetric structured emission profile of **A1**, with shoulders separated from the emission maximum by ~ 1100−1600 cm^{-1}, is not a mirror image of his structureless absorption spectrum. This suggests that the molecule is more planar in the excited state than in the ground state. If end dicyano substitution has no effect on the structured emission profile and lifetime of the excited state (1 ns), it increases the fluorescence quantum yield: 72% for **A3** as compared to 62% for **A1**. By another way, the di-*n*-hexyloxy substitution (see compound **A4**) or the replacement of the phenyl ring by a thienyl one (see compound **A2**), induces (i) a loss in the vibrational structure of the emission band with an increase of the Stokes shift, and (ii) a drastic decrease of the quantum yield (from 27 to 9.5%) and lifetime (from 0.77 to 0.47 ns) of the excited states for **A4** and **A2**, respectively. Since the Stokes shift is usually dependent on the solvent and the structural relaxation of the excited molecule, the solvent effect suggests that the charge distribution is more dissymmetric in the excited state and consequently that the dipole moment is larger for **A4** and **A2** than for **A1** and **A3**. Assuming that the electronic delocalization takes place over the molecule half between the pyridine and the end substituent, stabilization of the excited state depends on the strength of the donor: the stronger the donor, the greater the charge transfer between itself and the pyridine acceptor. Lower values of quantum yields for **B4** and **B2** (16 and 4% respectively) compared to those of **A4** and **A2** (27 and 9.5% respectively) confirm this hypothesis: introduction of the methyl group (donor character) as lateral substituent on the pyridinic ring increases even more the electronic density on the pyridinic ring. From these results, it can be deduced that the nonradiative deactivation processes of symmetrical molecules would be dependent on the electronic density of the pyridinic ring.

In the case of the donor−acceptor end-substituted chromophores (**A5** and **B5**), they display a broad and structureless longer wavelength fluorescence band. A large shift (~ 4500 cm^{-1}) in the position of the fluorescence maximum is also observed by varying the solvent polarity when dioxane is replaced by DMSO. The large solvatochromic effect is compatible with an emission originating from an intramolecular charge-transfer (ICT) state involving charge separation within the whole molecule. In this case, one electric charge is transferred from the donor moiety (*n*-hexyloxy) to the acceptor part of the molecule (cyano). Compared to symmetrical molecules, the charge localization is different: it occurs on the whole molecule, inducing consequently a larger dipole moment for the excited state.

Two other characteristics of the fluorescence of **A5** and **B5** are their high fluorescence quantum yield (50%) and long lifetime (2 ns) as compared to the corresponding values of the other chromophores. These data could be explained by a stabilization of the ICT state, which would involve structural modifications, such as rotations around molecular bonds. All these experimental results suggest that fluorescence occurs from a "twisted intramolecular charge transfer" (TICT) state for **A5** and **B5**, from a locally excited state with a planar geometry for the other symmetrical compounds. Note that **A5** and **B5** possess the same fluorescence quantum yield; this fact

Table 2. Optical Data of the Studied Compounds in a Toluene/Acetonitrile Mixture (50/50 v/v)

Compound	Absorption λ_{max} (nm) / E_{max} (eV)	Emission λ_{max} (nm) / E_{max} (eV)	Stokes Shift (nm)	Φ_f (%)	τ_f (ns)	k_f $(10\,\mu s)^{-1}$	Optical gap $E_{0\text{-}0}$ (eV)
A1	355 / 3.50	405 [a] / 3.08	50	62	0.98	63	3.20
B1	364 / 3.41	415 [a] / 3.00	51	58	1.07	54	3.12
A2	377 / 3.29	432 [a] / 2.93	55	9.5	0.47	20	3.02
B2	382 / 3.25	440 [a] / 2.81	58	4	0.39	10	2.95
A3	365 / 3.39	416 [a] / 3.02	51	72	1.0	72	3.12
B3	375 / 3.31	428 [a] / 2.91	53	71	1.16	61	3.03
A4	373 / 3.32	434 / 2.92	61	27	0.77	35	3.03
B4	378 / 3.28	440 / 2.80	62	16	0.68	23	2.98
A5	371 / 3.34	513 / 2.45	142	50	1.94	29	3.03
B5	379 / 3.27	520 / 2.42	146	51	2.01	26	2.94

[a] Only the wavelength of the highest energy shoulder is reported.
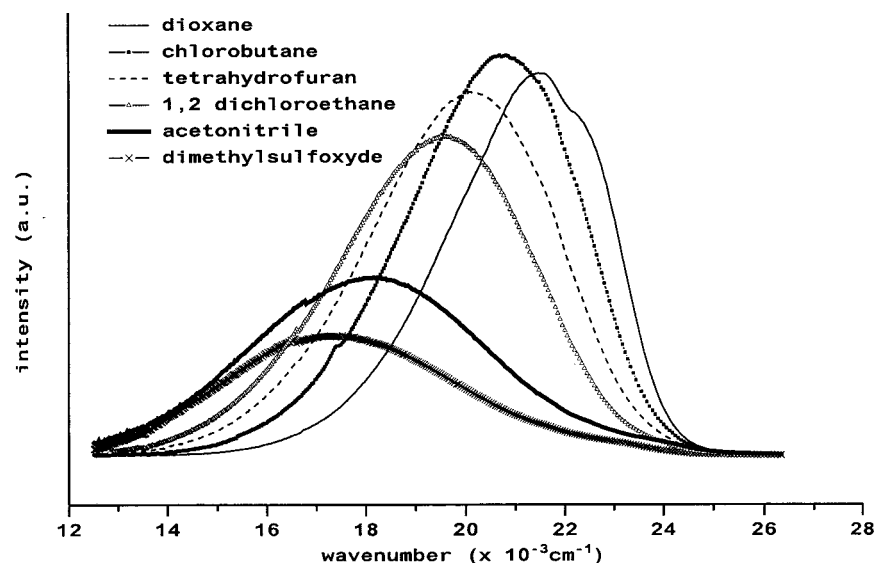
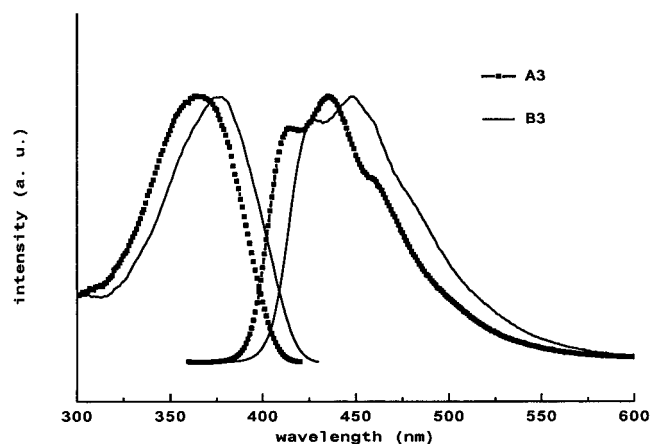**Figure 2.** Solvent effect on the emission spectra of **A5**.

Figure 3. Comparison of the absorption and emission spectra of **A3** and **B3** in toluene/acetonitrile mixture (50/50 v/v). Intensities of spectra have been normalized to the same value.

Figure 4. Comparison of the emission spectra of **A1**, **A3**, **A4**, and **A5** in (a) ethyl acetate solution and (b) in solid state.

confirms that their spectroscopic properties depend more on the end substituents than on the electronic density on the pyridinic ring.

Finally, the optical energy gaps $E_{0,0}$ determined by the 0,0 electronic transition energies are reported in Table 2. The gap is substantially decreased by the introduction of terminal or lateral substituent group. As $E_{0,0}$ is primarily governed by the conjugation length in the molecule, these results indicate an increase of the conjugation along the molecule backbones. The cyano group induces a lower effect than the donor groups as previously observed in the absorption and fluorescence measurements. Similarly a higher delocalization occurs when passing from phenyl- to thienyl-rings. For all the considered chromophores, the lateral methyl substituents on the pyridine induce a strong decrease of the optical gap.

3.3.2. Optical Study in Solid State. Photoluminescence experiments were carried out on powder. All compounds were examined, excepted **A2** and **B2** which exhibit low fluorescence quantum yield in solution. The emission spectra of **A1**, **A3**, **A4**, and **A5** in ethyl acetate (nonpolar solvent) and in solid state, are given in Figure 4 a and b, respectively.
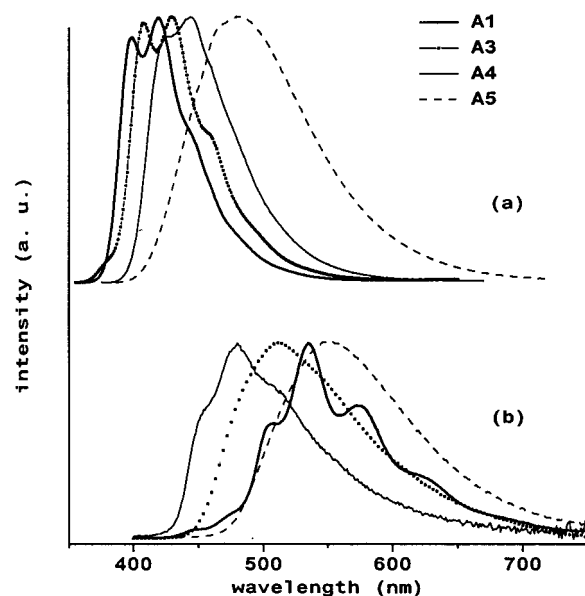
The first point evidenced in Figure 4 is that all the compounds display a red shift of their emission maxima on going from solution to the solid state. The second point is the existence of a structured emission for **A1** and **A3**, as observed in solution. **A1** exhibits a strong bathochromic shift ($\sim$6000 cm^{-1}) and a more structured emission profile than in solution, with well-defined features having a $\sim$1200 cm^{-1} energy separation. The large value of the observed shift can be identified as a Davydov shift, i.e., a splitting arising from the interactions between crystallographically nonequivalent molecules.[41] **A3**, **A4**, and **A5** give emission spectra red-shifted approximately 60, 15, and 25 nm, with poorer resolution. Except for **B1**, the introduction of the methyl lateral substituent on the pyridine, does not induce significant changes in the emission spectra. On the contrary, the shift is smaller for **B1** compared to **A1**, and also the emission spectra is less structured for **B1**

(41) Wright, J. D. *Molecular Crystal*; Cambridge University Press: Cambridge, 1995; pp 104–105.

than for **A1**, indicating that there is no Davydov splitting for the molecule with the lateral substituents (Figure 1S). This can be explained by an increase of disorder due to an increase of separation between molecules.[42]

3.4. Electrochemical Study. In view of the application of these molecules in optoelectronics, it is of interest to consider their energy gap—ΔE_g—and the relative ionization potential (IP) and electron affinity (EA). The ΔE_g value can be estimated from the difference between the first oxidation and first reduction potentials. These potentials are associated with the highest occupied and the lowest unoccupied molecular orbitals (HOMO and LUMO energy levels respectively), $\Delta E_g = E°_{ox1} - E°_{red1}$. This parameter will be compared to the energy 0,0 transition ($E_{0,0}$). Electrochemical measurements permit the estimation of the lifetimes of the generated ionic species. This allows the stability of the optoelectronics devices to be improved.

The electrochemical oxidation and reduction of the different distyryl-bipyridines have been investigated in toluene/acetonitrile mixture (50/50 v/v) (see Table 3). This mixture allows a good solubility (in the millimolar range in most cases) of the studied compound with retention of a sufficiently high conductivity as required for electrochemical studies. Typical voltammograms of the reduction and oxidation of the distyryl-bipyridines (as exemplified with **A1** and **B4**) are presented in Figure 5.

In reduction, all the studied compounds except **B3** present two monoelectronic transfers. The chemical stability of the different electrogenerated intermediates can be investigated just by considering the scan rate for which the cyclic voltammogram becomes reversible. The first reduction process was reversible at a low scan rate (0.2 V s^{-1}) showing a large chemical stability of the radical anion (lifetime on the order of 10 s). In these conditions, the second process can be unambiguously ascribed to the reduction of the radical anion to the corresponding dianion. The reversibility of the second reduction depends considerably on the substituents and was only observed at higher scan rates. For compounds with a donor group on the phenyl moieties (**A4**, **B4**) or thiophene (**A2**, **B2**), the second reduction becomes reversible for higher scan rates (100—200 V s^{-1}). When at least one acceptor group was present, the reversibility was observed at a much lower scan rate in the range of 0.2 V s^{-1}(for **A5** and **B5**). From these reversible voltammograms, the formal potentials $E°$ were immediately derived as the half-sum between the forward and the reverse scan peak potentials.[43] Both $E°$ were sensitive to the nature of substituents introduced on both sides of the molecules, indicating a good conjugation all along the molecule. As expected, a donor substituent like *n*-hexyloxy makes the potentials more negative and on the contrary, a cyano substituent renders the reduction easier. It is also noticeable that the difference between the first and second reduction potentials decreases considerably in the case of the dicyano compounds **A3**

and **B3**. For **B3**, the two reduction potentials were so close that only one large wave can be observed which impedes the determination of the individual $E°$. This phenomenon is indicative of an higher localization of the charge in the dianion in the vicinity of the two cyano groups than for the other studied compounds.

In oxidation, only one irreversible process has been observed. This peak remains irreversible even when the scan rate was increased up to several hundred volts per second, indicating that the lifetime of the produced radical cation is shorter than 1 ms in our experimental conditions. It is noticeable that the radical cation has a much lower chemical stability than the corresponding radical anion. In our determination, $E°_{ox}$ values (Table 3) were approximated by the corresponding peak potentials.

The electrochemical gaps range in the 2.7—3.3 eV. The ΔE_g and $E_{0,0}$ values are on the same order and follow the same general trends. The gap is substantially decreased by the introduction of a donor group (as terminal or lateral substituent). Introduction of a withdrawing group (cyano) does not much change the value of the gap, but increases the reduction potential.

To a first approximation, the oxidation potential can be related to the ionization potential and thus to the HOMO energy level.[44] According to this relation, the ionization potentials range in the 5.8—6.26 eV. A similar relationship can be made for the reduction potentials, the electron affinity and LUMO energies. All the compounds possess high electron affinity: **B4** has the lowest EA; **A3**, the highest one (2.84 and 3.19 eV respectively).

Substituent effect on formal reduction potentials of the compounds can be rationalized by the Hammett equation, i.e., by plotting $E°_{red1}$ versus the Hammett constant σ_p^-.[45] As shown in Figure 6, fairly good linear fitting of the experimental values can be obtained in the two series for the symmetrical compounds, with similar slopes, indicating an identical reduction mechanism and similar stabilization by mesomeric effects of the two types of generated radical anions. This result demonstrates the ability to tune, for symmetrical compounds, the reduction potential (electron affinity) through appropriate substitution by using the following relation. (For A series: $E°_{red} = -1.81 + 0.123\ \sigma_p^-$. For B series: $E°_{red} = -1.84 + 0.124\ \sigma_p^-$.) However, for donor—acceptor end-disubstituted molecules, the reduction potentials do not correlate with the Hammett coefficients σ_p^-. All these results can be related to those relative to the nature of the excited state, discussed in the previous part.

4. Conclusion

The present work has shown the ability to tune mesogenic, electrochemical, and optical (absorption—emission) properties of novel series of 6,6′-distyryl-3,3′-bipyridine derivatives, by variations in molecular design.

The compounds have been synthesized by Knoevenagel condensation of 6,6′-dimethyl-3,3′-bipyridine or
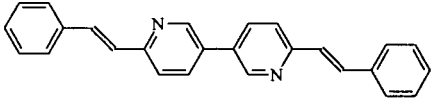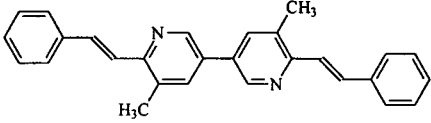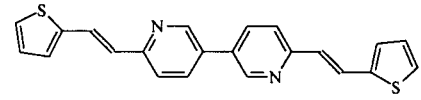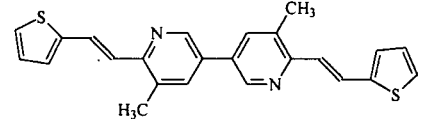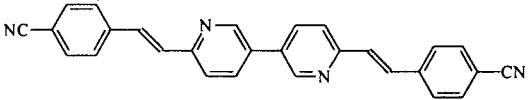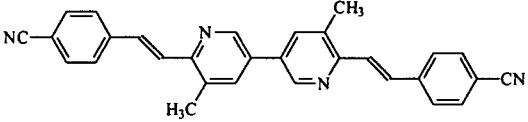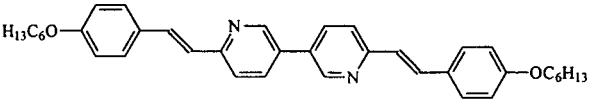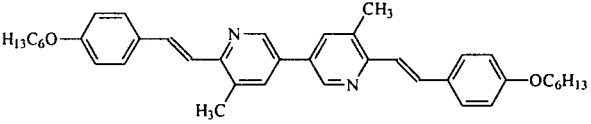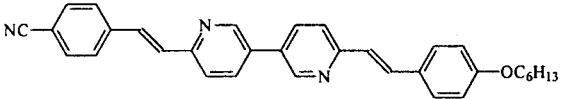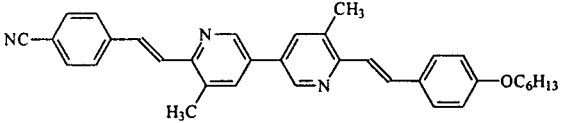
(42) Zerbi, G.; Castiglioni, C.; Del Zoppo, M. In *Electronic Materials: The Oligomer Approach*; Müllen, K., Wegner, G., Eds.; Wiley-VCH: Weinheim, 1997; p 345.

(43) Andrieux, C. P.; Savéant, J.-M. Electrochemical Reactions. In *Investigation of Rates and Mechanism of Reactions*; Bernasconi, C. F., Ed.; Wiley: New York, 1986; Vol. 6, 4/E, Part 2, pp 305—390.

(44) Moratti, S. C.; Bradley, D. D. C.; Cervini, R.; Friend, R. H.; Greenham, N. C.; Holmes, A. B. *SPIE* **1994**, *2144*, 108.

(45) Hansh, C.; Leo, A.; Taft, R. W. *Chem. Rev.* **1991**, *91*, 165.

Table 3. Electrochemical Data of the Studied Compounds in a Toluene/Acetonitrile Mixture (50/50v/v)

Compound	Oxydation E_{Ox}[b]	Reduction E^0_{red1}	E^0_{red2}	Electrochemical gap ΔE_g (V)[c]
A1	+1.52	-1.81	-1.94	3.33
B1	+1.37	-1.82	-2.03	3.19
A2	+1.18	-1.77	-1.97	2.95
B2	+1.18	-1.80	-2.01	2.98
A3	+1.61	-1.56	-1.62	3.17
B3	-[d]	-1.59[e]		-
A4	+1.11	-1.87	-2.01	2.98
B4	+1.07	-1.91	-2.16	2.98
A5	+1.23	-1.63	-1.82	2.86
B5	+1.10	-1.63	-1.84	2.73

The table header spans: Potential (V)[a] over Oxydation, Reduction; and Electrochemical gap.

[a] Versus SCE (see Experimental Section). [b] Peak potential. [c] $\Delta E_g = E_{ox} - E^{\circ}_{red1}$. [d] No oxidation wave has been observed [e] Two very close waves (see text).

5,5′,6,6′-tetramethyl-3,3′-bipyridine with aromatic aldehydes (thiophene or para-substituted phenyl).

n-Hexyloxy or cyano end substitutions favor the occurrence of smectic or nematic mesophases, whereas lateral disubstitution of the bipyridine core by methyl groups, decreases liquid crystal thermal stability. In the latter case, smectic phases are not demonstrated.

The redox potentials can be controlled through changes in the electron donor and acceptor character of the aromatic ring and/or of the end substituents. In all cases the molecules exhibit high electron affinity and large chemical stability of the radical anion. A good fit is
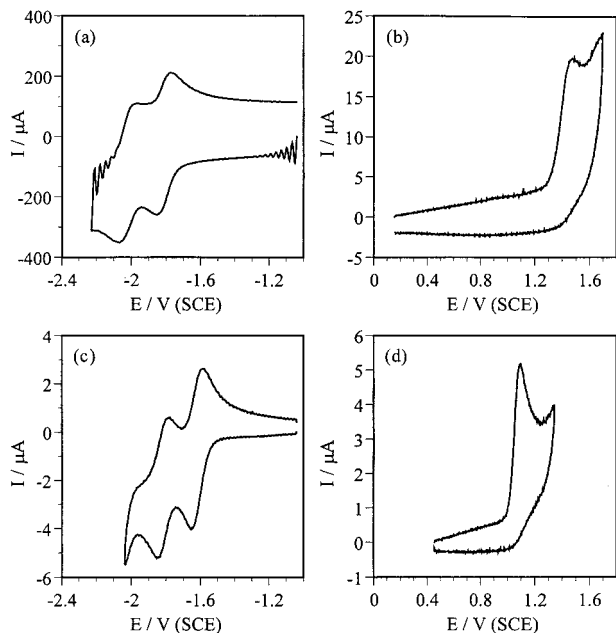
Figure 5. Cyclic voltammetry in toluene/acetonitrile mixture (50/50 v/v) containing 0.1 mol L^{-1} NBu_4BF_4 as supporting electrolyte on a 1-mm-diameter disk glassy carbon electrode: (a, b) **A1** concentration = 1.1 mol L^{-1}; scan rates v = 200 (a) and 0.2 (b) V s^{-1}; and (c, d) **B5** concentration = 1.0 mol L^{-1}; v = 0.2 V s^{-1}; T = 20 °C.
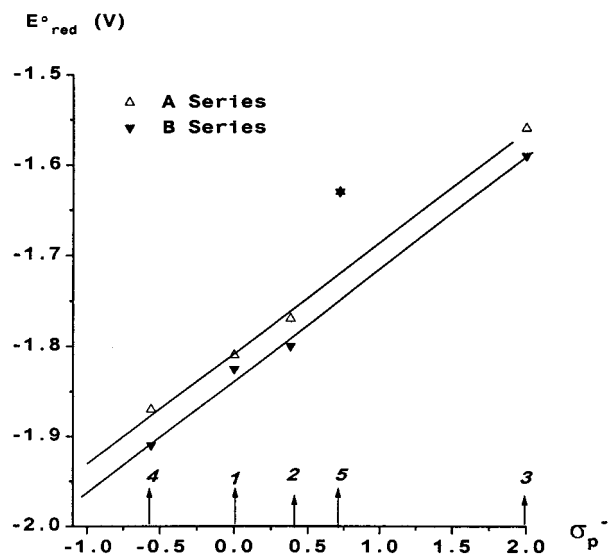

Figure 6. Variation of the formal reduction potentials of **A** and **B** series as a function of the Hammett coefficient σ_p^- in a toluene/acetonitrile mixture (50/50 v/v) containing 0.1 mol L^{-1} NBu_4BF_4 as supporting electrolyte.

obtained when the formal reduction potentials of the symmetrical compounds are plotted relative of the

Hammett constants σ_p^- of the substituents. These results should help us to develop chromophores that have desired electron affinity, which is of great interest for light-emitting diodes.

Absorption and emission energies on one hand, nature and lifetime of the excited state on the other hand can also be tuned through variations in the conjugated core or end substituents. In solution, symmetrical chromophores possess a planar excited state; the electron delocalization occurs on the molecule half, between the pyridine and the adjacent aromatic ring; the stronger the donor character of this latter, the lesser the stabilization of the excited state. Concerning dissymmetric chromophores with donor (*n*-hexyloxy) and acceptor (cyano) terminals groups, they exhibit an intramolecular charge-transfer excited state. In this case, a TICT mechanism could be expected.

These highly π-conjugated molecules open the way to applications in optoelectronics. This is especially the case with the donor−acceptor para-disubstituted compounds (**A5** and **B5**), which give rise to a charge-transfer phenomenon, allowing them to be active in NLO: optimization of the hyperpolarizability β and EFISHG measurements are under investigation. The photoluminescence, another property exhibited by most compounds, could be used for LEDs designing, as will be examined in a future paper.

If we consider the above-described molecules as model compounds, the versatility of the Knoevenagel condensation offers the opportunity to use (i) a wide range of aldehydes in order to improve some properties of interest, for example NLO properties, (ii) dialdehydes or aldehydes bearing reactive groups in order to synthesize main-chain or grafted polymers including such conjugated cores. For example, taking into account the formation of mesophases, the use of 4-hydroxybenzaldehyde offers the opportunity to synthesize reactive chromophores able to be grafted on macromolecular chain, with the purpose of obtaining side-chain liquid crystal polymers with NLO properties. This approach will be presented in a next paper.[46]

Supporting Information Available: Figure 1S, a comparison of the emission spectra of **A1** and **B1** in solid state. (Intensities of spectra have been normalized to the same value.) This material is available free of charge via the Internet at http://pubs.acs.org.

CM990501N

(46) Lemaître, N.; Attias, A.-J.; Noël, C. Manuscript in preparation.